ELSEVIER

PII: S0144-8617(96)00104-X

Carbohydrate Polymers 30 (1996) 135–140

0144-8617/96/$15.00 + .00

The network structure of gellan gum hydrogels based on the structural parameters by the analysis of the restricted diffusion of water

Akihiro Ohtsuka & Tokuko Watanabe*

Department of Food Science and Technology, Tokyo University of Fisheries, 4-5-7, Konan, Minato-ku, Tokyo 108, Japan

Gellan gum gels formed with potassium and calcium ions were investigated by the pulsed field gradient (PFG) stimulated echo NMR method. The structure of the gel network of the gellan gum gel was discussed on the basis of the interbarrier distance, a, the permeability of the barrier, p, and the actual diffusion coefficient of water, D_0. These structural parameters were estimated by the analysis of the restricted diffusion of water in the gel network. Three different types of gel, namely, weak gel, true gel and brittle gel, were obtained at various concentrations of the gel-promoting cation. Interestingly, the topological structure of the network in each type of gel as reflected by the structural parameters is identical in K^+-bridged gels and Ca^{2+}-bridged gels, although the absolute concentration of the cation needed to form the different network types is quite different. It is assumed that the binding structures at the crosslink and at the bridge between the helices are different between the type of cation. Nevertheless, structural properties of the network such as the average distance between junction zones and the permeability of the junction zone were independent of the type of gel-promoting cation. The change in the overall gel architecture formed by the junction zones in the gelation process seems to be identical in the cases of monovalent and divalent cations and the difference is only the gel-forming efficacy of cations. Copyright © 1996 Elsevier Science Ltd

INTRODUCTION

The microbial polysaccharide gellan gum, derived from *Pseudomonas elodea*, is a linear anionic polymer which consists of [,3)β-D-glucose, (1,4)β-D-glucuronic acid, (1,4)β-D-glucose, (1,4)α-L-rhamnose, (1,] repeating unit (Jansson *et al.*, 1983; O'Neil *et al.*, 1983). Carboxyl group in glucuronic acid is responsible for gelation in the presence of gel-promoting cations (Grasdalen & Smidsrod, 1987).

As to the gelation of gellan, it is commonly recognized that random coil–helix transition occurs prior to gelation, and then aggregation of the helices leads to the formation of junction zones (Grasdalen & Smidsrod, 1987; Dentini *et al.*, 1988; Morris, 1990; Yuguchi *et al.*, 1993; Yoshida & Takahashi, 1993). According to a schematic model by Morris (1990), end-to-end association of polymer chains via double helix formation upon cooling promotes fibrils and then gel-promoting cations promote inter-fibril and intra-fibre crystallization yielding crystalline junction zones, i.e. a permanent network. Formation of a dimer and a hexamer by side-by-side association was recently suggested from small angle X-ray scattering investigations (Yuguchi *et al.*, 1993, 1994; Yoshida & Takahashi, 1993).

Although the gelation mechanism on the microscopic scale refered to above has been extensively studied (Chandrasekaran *et al.*, 1988; Chandrasekaran & Thailambal, 1990; Chandrasekaran, 1991), the overall wide-gel 'architecture' has received less attention. The rheological properties of gels are strongly related to the connections between junction zones as well as the physicochemical properties of the junction zone. The properties of gellan gum gels are affected by the type of gel-promoting cation under the same gellan and cation concentrations (Morris, 1990; Moritaka *et al.*, 1991, 1992; Watase & Nishinari, 1993). Therefore, it is very important for a better understanding of gellan gum gels to characterize gel 'architecture' and gelation process under the various cation conditions. The overall 'architecture' will be termed the topological network structure in the text.

*Corresponding author.

We reported that the restricted diffusion of water in hydrogels and sols was informative for an elucidation of the gel and the sol structures, that is, the size of water cluster, diffusibility of water between junction zones and permeability of the junction zone (Ohtsuka *et al.*, 1994; Watanabe *et al.*, 1996; Watanabe & Ohtsuka 1993).

In the present paper, the translational diffusion of bulk water in the gel network was measured by the pulsed field gradient NMR method and the diffusion time dependence of the observed restricted diffusion was analyzed to evaluate the gel structure over micron to 10 micron scales. From the relative changes of the permeability of the diffusion barrier and the average distance between diffusion barriers, three types of gellan gum gel, i.e. weak, true and brittle gels, were distinguished.

MATERIALS AND METHOD

Sample preparation

Gellan gum (in powder form), so called sodium-type, was donated from Kelco Division of Merck & Co. Inc., CA, USA. The contents of cations contained in the original powder were determined by Kelco as follows; Na^+, 3.03%, K^+, 0.19%, Ca^{2+}, 0.11%, Mg^{2+}, 0.02%. The amount of the originally included cation was counted in the cation concentration of the sol and the gel samples under investigation. Therefore, the minimum concentrations of K^+, Na^+ and Ca^{2+} ions are 0.97 mmol/1000 g, 26.3 mmol/1000 g and 0.55 mmol/1000 g, respectively, in 2 w/w % of the gellan gum solution.

Gellan gum powder was suspended in ion exchanged distilled water. The suspension was held at 40°C overnight to swell sufficiently. It was heated and stirred at 70°C for 2h and at 90°C for 1h to dissolve completely. A significant amount of an aqueous solution of potassium chloride or calcium chloride was added to the gellan gum solution at 90°C. Gellan gum concentration was fixed as 2 w/w % in all samples, and the final concentrations of K^+ and Ca^{2+} ions were in the range of 10–90 and 1.7–5.9 mmol/1000 g, respectively. All samples were held at room temperature for 4 days prior to NMR measurement.

Diffusion measurement of water

The pulsed field gradient stimulated echo (PFGSTE) pulse sequence for diffusion measurement (Tanner, 1970) was used. The details were described in a previous paper (Ohtsuka *et al.*, 1994). The parameters were set as follows: the magnitude of the field gradient pulse, g~50–500 mT/m, the diffusion time, Δ~60–610 ms, and duration of field gradient pulse, $\delta = 1$ ms. The $\pi/2$ pulse width was determined for the water proton in each sample and was in the range 8.9 9.4μs. The accumulation number of the scans was 8 for each measurement. Spectral width was set to 5000Hz. Measurement was carried out by using an MSL100 spectrometer (Bruker) at 23°C. The stimulated echo signal was Fourier-transformed to obtain the signal amplitude of water.

The ratio of the amplitude in the presence of the field gradient to that in the absence of the field gradient, R, is expressed in eqn (1):

$$\ln[R] = -D(\gamma\delta g)^2\left(\Delta - \frac{\delta}{3}\right). \quad (1)$$

Diffusion coefficient was calculated from the slope of $\ln[R]$ vs $(\gamma\delta g)^2(\Delta-\delta/3)$ plot by stepwisely changing g for each diffusion time, Δ. If the diffusion of water is restricted, the observed diffusion coefficient shows a diffusion time dependence.

RESULTS

Fig. 1(A) shows the relationship between $\ln[R]$ and $(\delta g)^2(\Delta-\delta/3)$ in the case of the 2w/w% gellan gum gel with 25mmolK^+/1000g. A series of $\ln[R]$ vs $(\delta g)^2(\Delta-\delta/$

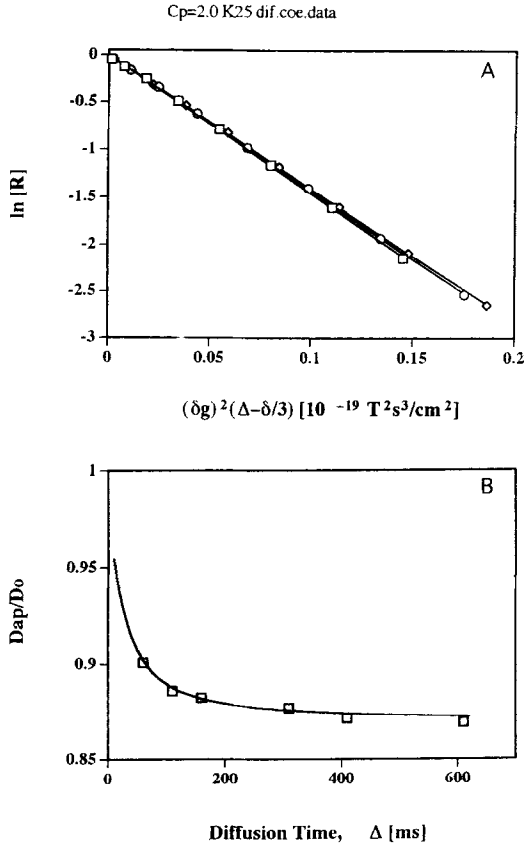

Fig. 1. Diffusion time dependence of signal attenuation of water in 2w/w% gellan gum gel with 25mmolK^+/1000g. (A) $\ln[R]$ vs $(g\delta)^2(\Delta-\delta/3)$ plotted at $\Delta = 60$ (□), 110 (○) and 410ms (◇). Solid lines were calculated by least square fitting of the observed data points. (B) D_{ap}/D_0 vs Δ plot. Solid line corresponds to the least squares fitted curve from eqn (2) in the text.

3) plots showed a good linearity for each Δ. The data indicate that there exists only one type of diffusion component in the sample under the present experimental conditions.

The apparent diffusion coefficient, D_{ap}, i.e. the slope, sequentially decreased with increasing Δ, which means that diffusion of water in the gellan gum gels is restricted. The difference between D_{ap} for each Δ value was very small but significant in comparison with an average standard deviation in our experiment. All other samples showed similar results. Very high precision is required in measurement.

In order to evaluate an actual diffusion coefficient from the apparent diffusion coefficient, we applied the rather simple model presented by Tanner (1978) and modified by von Meerwall & Ferguson (1981), in which permeable barriers are parallel to each other and separated by the same distance. Diffusion phenomena in such geometry are described by eqn (2):

$$R(t) = \exp\left[-\frac{\theta^2 D_0 t}{a^2}(\sin^2\alpha + A)\right]\frac{2}{\pi^2 d^2} \left\{1 - \cos\pi d + 2\sum_{n=1}^{m}\left[\frac{1-(-1)^n\cos\pi d}{(1-n^2/d^2)^2}\right.\right. \exp\left.\left.\left(-\frac{n^2\pi^2 D_0 B t}{a^2}\right)\right]\right\} \quad (2)$$

where t is the diffusion time, a, distance between barriers, D_0, the interbarrier diffusion coefficient, α, the angle between the barrier and the direction of the principal axis of the field gradient and $\theta = \gamma g \delta a$, $d = (\theta/\pi)|\cos\alpha|$. The reduced permeability, P is expressed to $P = ap/D_0$, where p is the permeability of the barriers. The coefficients A and B correspond to $\cos^2\alpha/(1 + 1/P)$ and $1/(1 + P)$, respectively. The structural parameters (a, p, D_0) were obtained by fitting eqn (2) to the observed data. Fig. 1(B) shows a typical example of data fitting for the sample shown in Fig. 1(A), where the ratios of D_{ap} to D_0 were plotted against the diffusion time. The calculated curve (solid line in Fig. 1(B)) shows a good agreement with the observed values as $D_0 = 2.267 \times 10^{-5}$cm^2/s, $a = 7.5$μm, $P = 6.63$ ($p = 0.20$cm/s). The structural parameters and the interbarrier diffusion coefficients estimated for the various gels are plotted in Figs 2 and 3 against the concentration of K^+ and Ca^{2+} ions, respectively.

DISCUSSION

Actual diffusion coefficient of water in the gellan gum gels

Reduction of the apparent diffusion coefficients of bulk water with increasing diffusion time suggests a restriction in the diffusional motion of water by the gel network. As shown in Figs 2(A) and 3(A), however, the

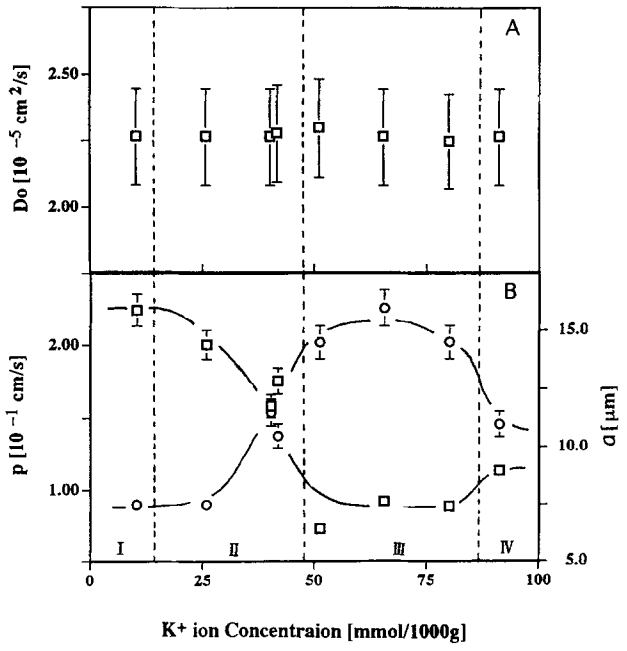

Fig. 2. K^+ concentration dependence of (A) diffusion coefficient of water, D_0, and (B) size of water compartment, a (○), and permeability of gel network, p (□). Zone I, II, III and IV correspond to the states of sol, weak gel, K^+-bridged true gel and brittle gel, respectively (see text).

values of the actual diffusion coefficient of water, that is, interbarrier diffusion coefficient, D_0, in gellan gum gels investigated were thus far identical and averaged 2.25×10^{-5}cm^2/s. This value is almost equal to the self-diffusion coefficient of pure water, 2.3×10^{-5}cm^2/s at 23°C (Mills & Lobo, 1989), that is, diffusional mobility of water in the gellan gum gels is much the same as pure water. The existence of the loose end of polymer in bulk water in the network was assumed in the model proposed by Morris (1990). The present result suggests that there exists no loose end of polymer, or its amount is too little to become an obstruction for water diffusion in the gellan gum gels (2.0w/w% gellan gum concentration). As we will discuss later, in the K^+-gel, the gelation does not occur at concentrations of K^+ ions below about 50mmol/1000g and is gradually promoted with increasing cation strength. Therefore, it is certain that the loose end of the polymer and/or double helices, which are not included in the junction zone, exist as solute in the water pool.

The structural change in the K^+-bridged gellan gum gel

Values of a and p symmetrically changed with increasing K^+ ion concentration (see Fig. 2(B)). In the sol state (10mmolK^+/1000g), the value of a was small (7–8μm) and the value of p was large (0.22cm/s) in comparison with those in the gel states. This property of p and a, that is, $a(\text{sol}) < a(\text{gel})$ and $p(\text{sol}) > p(\text{gel})$, is a common characteristic feature in various sol and gel systems (Watanabe *et al.*, 1996; Watanabe & Ohtsuka, 1993). For

the samples including K^+ ion in the range of 25–50mmol/1000g, the gels formed were rather soft (low elastic). A gradual change in the values of *a* and *p* started from the specific values of the sol state to larger *a* values and to smaller *p* values with increasing K^+ ion concentration. This change in the structural parameters suggests a further promotion of gelation via large amounts of K^+ ions. The aggregation of the double helices through K^+ ions leads to an increase in the void space and to a higher density of junction domains, i.e. less permeability. At K^+ ion concentration of about 50mmol/1000g, *a* and *p* reached the maximum and minimum values (a~15μm and p~0.095cm/s), respectively, and remained nearly constant as the concentration increased to 80mmol/1000g. All gels formed in this concentration range were transparent and viscoelastic. At concentrations of 90mmol/1000g K^+ ions opaque gels formed and, an abrupt change in *a* and *p* was observed. The value of *a* decreased dramatically as the value of *p* increased, compared with the transparent elastic gels. It is known that an excess of cation leads to opaque and inhomogeneous gels (Grasdalen & Smidsrod, 1987).

From the change in the estimated structural parameters, we divided the gelation process via K^+ ions into four zones, I to IV, as shown in Fig. 2(B). Zone I is the sol phase. Zone II is the first step of gelation in which so called 'weak gels' were formed. In the weak gels both a sol-like phase (partially free double helix) and a gel-like phase (aggregation of the double helices) coexist as a mixture and a fraction of the gel-like phase increases with increasing number of coexisting K^+ ions from 10 to 50mmol/1000g. Consequently, the permeability of the diffusion barrier gradually decreases and the inter-barrier space increases as gelation proceeds. Increase in the amount of junction zone with cation strength was suggested by the rheological studies (Moritaka *et al.*, 1991; Watase & Nishinari, 1993). In zone III (K^+ ion concentration from 50 to 80mmol/1000g), the formation of the elastic gels was completed and addition of K^+ ions induces no significant changes in the gel structure, as shown by the nearly constant values of *p* and *a*. Water proton relaxation rates in these gels showed constant values (unpublished data). Constancy of *p* and *a* as well as relaxation times suggests that additional K^+ does not contribute to the crystalline junction zone. We define the gel in the zone III as a 'K^+-bridged true gel'. Excess cations might be trapped in a cage between double helices and a cage within a helix by replacement of hydrated water (Chandrasekaran, 1991; Watanabe *et al.*, 1996). The structural parameters of the gel formed in zone IV suggest that the crystalline junction zone becomes loose and partial separation of polymer chains from the multistrand junction zone occurs in the opaque gels. Zone IV corresponds to the third step in the K^+-promoting gelation process where a phase separated brittle gel is formed. Detail of zone IV will be discussed in the next paragraph.

The network structure in the Ca^{2+}-bridged gellan gum gel

As shown in Fig. 3(B), a gelation process via Ca^{2+} ions is divided into the two zones, I and II. Elastic gels were formed by 1.6–3.2mmol/1000g of Ca^{2+} ions (zone I) and these gels showed identical values of *a* (ca. 15μm) and *p* (ca. 0.095cm/s), which indicates that they have an identical network structure in spite of the difference in the cation concentration. Notice that this situation is the same with the above-mentioned zone III K^+-bridged gel. Therefore, in the same manner as for the K^+-bridged true gel, we define the gels in zone I as 'Ca^{2+}-bridged true gel'. A higher amount of Ca^{2+} ions in the range of 3.5–5.9mmol/1000g (zone II) induced opaque gels, of which the value of *a* decreases abruptly and the value of *p* increases slightly compared with those of the true gel. The structural parameters were the same in all gels formed by higher Ca^{2+} ion concentrations (a~11μm and p~1.15cm/s). The structural change between zone I and zone II in the Ca^{2+} system was equivalent to that between zone III and zone IV in the K^+ system, that is, the change from the true gel to the brittle gel. Therefore, the gels formed in zone II in the Ca^{2+} system were assumed to have the same topological network structure as the K^+-bridged brittle gel.

2w/w% gellan gum solutions contained 0.55mmol/1000g Ca^{2+} as the original sample included 0.11% of Ca^{2+} ion. Gellan solutions containing 0.55mmol/1000g of Ca^{2+} ion were in the sol state and gellan solutions with 1.6mmol/1000g of Ca^{2+} ion formed a true gel, as

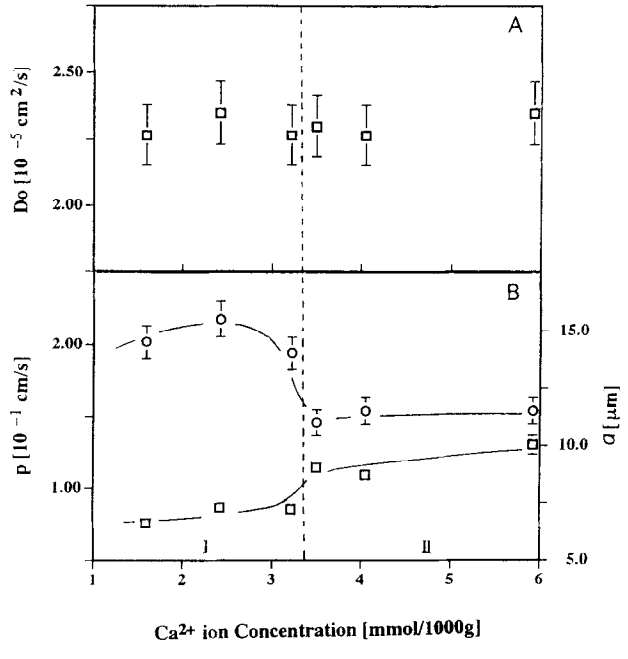

Fig. 3. Ca^{2+} concentration dependence of (A) diffusion coefficient of water, D_0, and (B) size of water compartment, *a* (○), and permeability of gel network, *p* (□). Zone I and II correspond to Ca^{2+}-bridged true gel and brittle gel, respectively (see text).

mentioned above. In the present investigation the weak gel forming zone via Ca^{2+} ions was not detected, but we could observe the process over a very narrow concentration range under appropriate conditions.

The gelation process and the topological network structure in gellan gum gels

The formation of three different types of gel, i.e. weak gel, true gel and brittle gel, was recognized in the gelation process via both cations. If we compare the absolute values of the structural parameters for the two cations they superimpose for an appropriate cation concentration shift, as shown in Fig. 4. Namely, the structural property estimated by the analysis of the restricted diffusion of water in each gel state does not depend on the identity of cation, but depends on the cation concentration. In this investigation the network structure is considered as a diffusion-barrier for water. The structural property mentioned above is associated with the topological structure between junction zones rather than the microstructure of the crosslink and the interchain structure.

The crystal structures of gellan and its potassium salt were investigated by X-ray diffraction analysis of oriented fibers (Chandrasekaran *et al.*, 1988). According to their result, the gellan molecule forms a parallel, half-staggered, double helix and the potassium ion is coordinated to the hydroxyl group, which is in turn involved in interchain hydrogen-bonds to stabilize the duplex. Furthermore, two such duplexes are packed antiparallel to each other, and crosslinked by a network of duplex–water–duplex interactions. While, in the calcium salt, the structure was extrapolated by computer modeling (Chandrasekaran, 1991). The carboxyl group–calcium ion–carboxyl group directly crosslinks adjacent gellan molecules (Chandrasekaran & Thailambal, 1990; Chandrasekaran, 1991). It is quite interesting that the topological network structure on the ten micron scale is identical in both K^+ and Ca^{2+}-bridged gellan gum gels, although the microstructures of the crosslink are different from each other. This would be because the basic size of one strand and the distance between strands in the multistrand junction zone are determined by the helical structure of gellan molecules which is independent of cation and because cations just replace the position of the hydration water molecules between the helices.

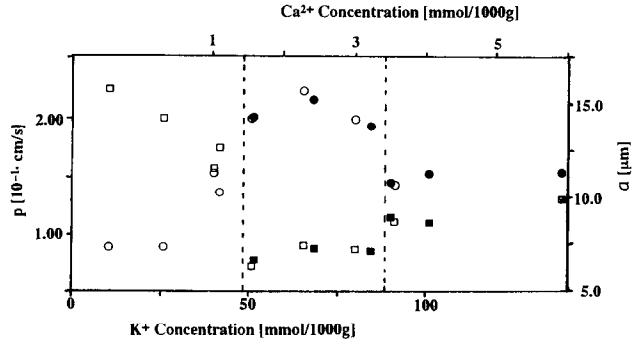

Fig. 4. Characteristic structural parameters, a (○,●) and p (□,■) in the gelation process of gellan gum gel via cations. Open symbols and filled symbols correspond to potassium added system and calcium added system, respectively.

CONCLUSION

It was shown that the characteristic feature of the sol and the gel states is reflected in the structural parameters which are obtained from analyzing the restricted diffusion of water and that the structural parameters are very useful for following the structural change in the gelation process. Specifically, a feature of the sol state was represented as small a and large p, and the value of a became larger and the value of p became smaller as gelation progressed to reach their maximum and the minimum values, respectively (Figs 2(B) and 3(B)).

According to the change of the structural parameters, the gelation process is explained as follows. In the sol state, the gellan gum chains are known to distribute homogeneously as random coil and/or double helices (Upstill *et al.*, 1986; Grasdalen & Smidsrod, 1987). The present result suggests that momentary crosslinks between gellan molecules and therefore momentary network structures are generated by cations even in the sol state, but they are too weak to be maintained against thermal motion. The existence of enough cation induces aggregation of the helices to form junction zones, i.e. gel formation. If the number of the cations is not enough, a weak gel is formed, where the sol-like phase and the gel-like phase coexist and some carboxyl groups are free from the junction zone. With an increase of cation concentration the proportion of the gel-like phase increases resulting in the formation of a true gel. In true gels the majority of the carboxyl groups contribute to the junction zones and water molecules move in the space between junction zones like free water (Figs 2(A)–3(A)). A large excess of cation induces the formation of brittle gels which are opaque and inhomogeneous. As for the gelation of the brittle gels, we assume two routes, one is the aggregation of the double helices and the other is an intramolecular crosslinking process. The former forms junction domains such as observed in the true gel and the latter forms intramolecular aggregation of the random coil because of neutralization of the negative charges. These two types of aggregation of gellan proceed simultaneously at high cation concentrations and high sample preparation temperatures.

In the gelation process with various concentration of cation, three different types of gel were recognized on the basis of the restricted diffusion of water. The topological structure of the three-dimensional network was

identical between K^+-bridged gels and Ca^{2+}-bridged gels in all types of gel, that is, no cation-type dependency was observed in the gel structure. It is known that the rheological nature of gellan gum gels is independent of the kind of cations but depends on the cation concentration (Sanderson & Clark, 1983). For TMA–gellan gum in TMACl, the plot of the intrinsic viscosities against the reciprocal of the root of the ionic strengths showed different behaviors in three different ranges of ionic strength, which are referred to as the chain-contracting zone, the chain-ordering zone and the chain-association zone, respectively (Grasdalen & Smidsrod, 1987). It would be interesting to make a clear correlation between the topological gel structure and the rheological properties which would contribute to a better understanding of the cation specific properties of gellan gum gels.

If we calculate the molar number of the repeat unit in 2w/w% gellan solution, the concentration of the repeat unit is about 30mmol[$C_{24}H_{38}O_{20}$]/1000g. Therefore, about 30mmol/1000g of K^+ ion is enough to saturate the binding to COO^- groups in the polymer chains, because each repeat unit has one carboxyl group. Actually, 50mmol/1000g of K^+ ions or 1.6mmol/1000g of Ca^{2+} ions were the lowest concentration required to form a true gel. The number of Ca^{2+} ions needed to form the Ca^{2+}-bridged true gel is much less than the number of carboxyl group in the system. It has already been made clear that the effectiveness of crosslink formation is different between both cations, but it is a new finding of the present work that both cations form identical topological structures in the gel network.

ACKNOWLEDGEMENTS

This work has been supported in part by a grant from the National Institute for Physiological Sciences, Okazaki, Japan.

REFERENCES

Chandrasekaran, R., Puigjaner, L.C., Joyce, K.L. & Arnott, S. (1988). *Carbohydr. Res.*, **181,** 23–40.

Chandrasekaran, R. & Thailambal, V. G. (1990). *Carbohydr. Polym.*, **12,** 431–442.

Chandrasekaran, R. (1991). *Water Relationships in Food*, eds H. Levine & L. Slade. Plenum Press, New York, pp. 773–784.

Dentini, M., Coviello, T., Burchard, W., Crescenzi, V. (1988). *Macromolecules,* **21,** 3312–3320.

Grasdalen, H. & Smidsrod, O. (1987). *Carbohydr. Polym.*, **7,** 371–393.

Jansson, P., Lndberg, B. & Sandford, P. A. (1983). *Carbohydr. Res.*, **124,** 135–139.

O'Neil, M. A., Selvendran, R. R. & Morris, V. J. (1983). *Carbohydr. Res.*, **124,** 123–133.

Mills, R. & Lobo, V. M. M. (eds) (1989). *Self-Diffusion in Electrolyte Solutions.* Elsevier, New York.

Morris, V. J. (1990). *Food Polymer Gels, and Colloids*, ed. E. Dickinson, Special Publication 82. Royal Soc. Chem., UK, pp. 310–321.

Moritaka, H., Fukuba, H., Nakahama, N. & Nishinari, K. (1991). *Food Hydrocolloids,* **7,** 457–458.

Moritaka, H., Nishinari, K., Nakahama, N. & Fukuba, H. (1992). *Biosci. Biotech. Biochem.*, **56,** 595–599.

Ohtsuka, A., Watanabe, T. & Suzuki, T. (1994). *Carbohydr. Polym.*, **25,** 95–100.

Sanderson, G. R. & Clark, R. C. (1983). *Food Technol.*, **April,** 63–70.

Tanner, J. E. (1970). *J. Chem. Phys.*, **52,** 2523–2526.

Tanner, J. E. (1978). *J. Chem. Phys.*, **69,** 1748–1754.

von Meerwall, E.Ferguson, R. D. (1981). *J. Chem. Phys.*, **74,** 6656–6659.

Watanabe, T. & Ohtsuka, A. (1993). *Molecular Environment of Intra- and Extracellular Sodium*, eds Y. Seo et al., Seiriken, Okazaki, pp. 77–80.

Watanabe, T., Ohtsuka, A., Murase, N., Barth, P. & Gersonde, K. (1995). *Magn. Reson. Med.*, **35,** 697–705.

Watase, M. & Nishinari, K. (1993). *Food Hydrocolloids,* **7,** 449–456.

Yoshida, Y. & Takahashi, M. (1993). *Food Hydrocolloids,* **7,** 387–395.

Yuguchi, Y., Mimura, M., Kitamura, S., Urakawa, H. & Kajiwara, K. (1993). *Food Hydrocolloids,* **7,** 373–385.

Yuguchi, Y., Mimura, M., Urakawa, H. & Kajiwara, K. (1994). *Polym. Prepr., Jpn,* **43,** 2689–2690.